ALMA MATER STUDIORUM
UNIVERSITÀ DI BOLOGNA

ARCHIVIO ISTITUZIONALE
DELLA RICERCA

Alma Mater Studiorum Università di Bologna
Archivio istituzionale della ricerca

Design, synthesis and biological profile of new inhibitors of multidrug resistance associated proteins carrying a polycyclic scaffold

This is the final peer-reviewed author's accepted manuscript (postprint) of the following publication:

Published Version:
Alessandra, B., Silvia, G., Lucia, M., Giovanna, F., Federica, B., Angela, R., et al. (2015). Design, synthesis and biological profile of new inhibitors of multidrug resistance associated proteins carrying a polycyclic scaffold. EUROPEAN JOURNAL OF MEDICINAL CHEMISTRY, 92, 471-480 [10.1016/j.ejmech.2015.01.004].

Availability:
This version is available at: https://hdl.handle.net/11585/491974 since: 2020-02-18

Published:

DOI: http://doi.org/10.1016/j.ejmech.2015.01.004

Terms of use:

Some rights reserved. The terms and conditions for the reuse of this version of the manuscript are specified in the publishing policy. For all terms of use and more information see the publisher's website.

This item was downloaded from IRIS Università di Bologna (https://cris.unibo.it/).
When citing, please refer to the published version.

(Article begins on next page)

21 March 2025

This is the final peer-reviewed accepted manuscript of:

Bisi, A.; Gobbi, S.; Merolle, L.; Farruggia, G.; Belluti, F.; Rampa, A.; Molnar, J.; Malucelli, E.; Cappadone, C. Design, synthesis and biological profile of new inhibitors of multidrug resistance associated proteins carrying a polycyclic scaffold. Eur. J. Med. Chem., 2015, 92, 471-480.

The final published version is available online at:

https://doi.org/10.1016/j.ejmech.2015.01.004

Rights / License:

The terms and conditions for the reuse of this version of the manuscript are specified in the publishing policy. For all terms of use and more information see the publisher's website.

This item was downloaded from IRIS Università di Bologna (https://cris.unibo.it/)

When citing, please refer to the published version.

Design, synthesis and biological profile of new inhibitors of multidrug resistance associated proteins carrying a polycyclic scaffold.

Alessandra Bisi,*[a] Silvia Gobbi,[a] Lucia Merolle,[b] Giovanna Farruggia,[b,c] Federica Belluti,[a] Angela Rampa,[a] Joseph Molnar,[d] Emil Malucelli,[b] Concettina Cappadone[b]

Department of Pharmacy and Biotechnology, Alma Mater Studiorum University of Bologna [a]Via Belmeloro, 6, 40126 and [b]Via S. Donato, 19/2, 40127, Bologna, Italy, [c]National Institute of Biostructures and Biosystems, Via delle Medaglie D'oro, 305, 00136, Roma, Italy, [d]Institute of Medical Microbiology and Immunobiology, Faculty of Medicine, University of Szeged, Szeged, Hungary.

*Corresponding author:

Alessandra Bisi

Phone: +39 051 2099710

Fax: +39 051 2099734

Email: alessandra.bisi@unibo.it

Abstract

Following the identification of a novel polycyclic scaffold, leading to the previously reported potent P-gp modulator **1**, a small series of easily affordable derivatives bearing a properly selected nitrogen-containing but-2-ynyl side chain was now synthesized and tested to evaluate the MDR reverting activity on two different experimental models. All compounds proved not to be cytotoxic when tested alone and more potent chemosensitizers than the reference verapamil. Some of them showed remarkable effects in combination with doxorubicin, being able to induce apoptotic cell death due to their reverting activity. In particular, **2a** and **2c** could be regarded as non-toxic new potential chemosensitizers, being able to interfere with different ABC proteins. Moreover, the intrinsic cytotoxicity of compound **1** could broaden its employment as MDR modulator. These results also seem to confirm the polycyclic core of these compounds as a potential new pharmacophoric carrier in medicinal chemistry.

Keywords: P-glycoprotein; MDR-1; MDR modulators; chemosensitizers; anticancer;drug design

1. Introduction

Cancer is a hyperproliferative disease mainly characterized by transformation, dysregulation of apoptosis, angiogenesis, invasion and metastasis. Chemotherapy has been introduced into treatment strategies in the last few decades and it is well known that the effects of most classical antiproliferative agents could be related to an impairment in cell cycle progression [1]. The cell cycle is composed of a series of tightly integrated events that allow the cell to grow and proliferate. With the new progresses in understanding the basic molecular mechanisms underlying cell cycle regulation and apoptosis and how these processes are impaired in tumor cells, recent research has been addressed to identify molecules capable of directly interfering with the specific intracellular targets involved, such as cyclines, cycline-dependent kinases (CDKs), B-cell lymphoma-2 (Bcl-2), inhibitors of apoptotic proteins (IAPs), etc. [2-4]. Although the improvement in cancer therapies resulted in the discovery of new drugs and new therapeutic strategies, the onset of chemoresistance severely limits their area of application. In the last decades many efforts have been made to identify new experimental strategies to overcome this problem, involving the development of novel reversal agents (chemosensitizers) or drugs capable of killing resistant cells.

Several different mechanisms are involved in the development of resistance to chemotherapy, such as decreased uptake of water-soluble drugs, increased DNA damage repair, altered drug metabolism, reduced apoptosis, and increased ATP-dependent efflux of hydrophobic anticancer agents that enter the cells by diffusion through the plasma membrane. This last phenomenon is known as multidrug resistance (MDR) and is the major and still unsolved clinical problem in the treatment of cancer [5]. MDR can arise *de novo* or after exposure of cancer cells even to a single drug and is characterized by cross resistance to a series of structurally unrelated compounds with different subcellular targets. Well characterized mechanism contributing to MDR is the overexpression of membrane efflux pumps, belonging to the evolutionarily conserved family of ATP binding cassette (ABC) proteins, which transport anticancer drugs out of the cells so that

effective intracellular drug levels are no longer reached. In humans, more than 48 MDR genes were identified from the ABC transporter superfamily, among which the most extensively characterized MDR transporters include P-glycoprotein (P-gp/ABCB1) and multidrug resistance associated protein-1 (MRP1/ABCC1) [6,7]. The constitutive expression of these proteins occurs in hematopoietic cells of peripheral blood, lung, testicle, placenta, brain, kidneys, adrenal gland, duodenum, heart, colon, and skeletal muscle [8]. These transporters play an important physiological role in detoxifying cells from both metabolites produced by normal cellular processes and exogenous toxic agents, such as chemotherapy drugs, which favours the resistance mechanism [9,10].

P-gp is a 170 kDa protein, classified, from a structural viewpoint, as a pseudosymmetrical heterodimer, where each monomer consists of six transmembrane domains (TMD), which is responsible for the recognition and transport of substrates, and one nucleotide-binding domain (NBD) for ATP binding and hydrolysis [11]. MRP1 is a 190 kDa protein consisting of 17 TMD having P-gp like cores, mainly located in the plasma membrane. MRP1 acts as an ATP-dependent glutathione S-conjugate export pump (GS-X pump), thus its MDR mechanism is entirely different from that of P-gp mediated resistance. However, many of the anticancer drugs which are substrates for P-gp are also substrates for MRP1 [12].

Nowadays, the most accepted strategy to overcome ABC-cassette mediated drug resistance consists in the co-administration of the anti-cancer drug with a reversal agent, capable of inhibiting its efflux from the cell. However, this strategy shows some drawbacks, related to both the functional role of these transporters in healthy tissues and the possibility of unpredictable drug-drug pharmacokinetics interactions. The P-gp drug binding site is indeed similar to the binding site of CYP3A4, leading to a possible concurrent inhibition of this enzyme, thus interfering with the intestinal or liver metabolism of the anticancer drug [13] A wide variety of natural and synthetic compounds with the properties of inhibiting P-gp have been described to date, from the calcium antagonist verapamil

(Figure 1), one of the first generation reversal agents, to the more specific potent third generation MDR modulators. Among these, the most promising proved to be tariquidar (XR9576) [14] and zosuquidar (LY335979) [15] (Figure 1), which showed minimal pharmacokinetic interactions. They have entered clinical trials but to date are not clinically available.

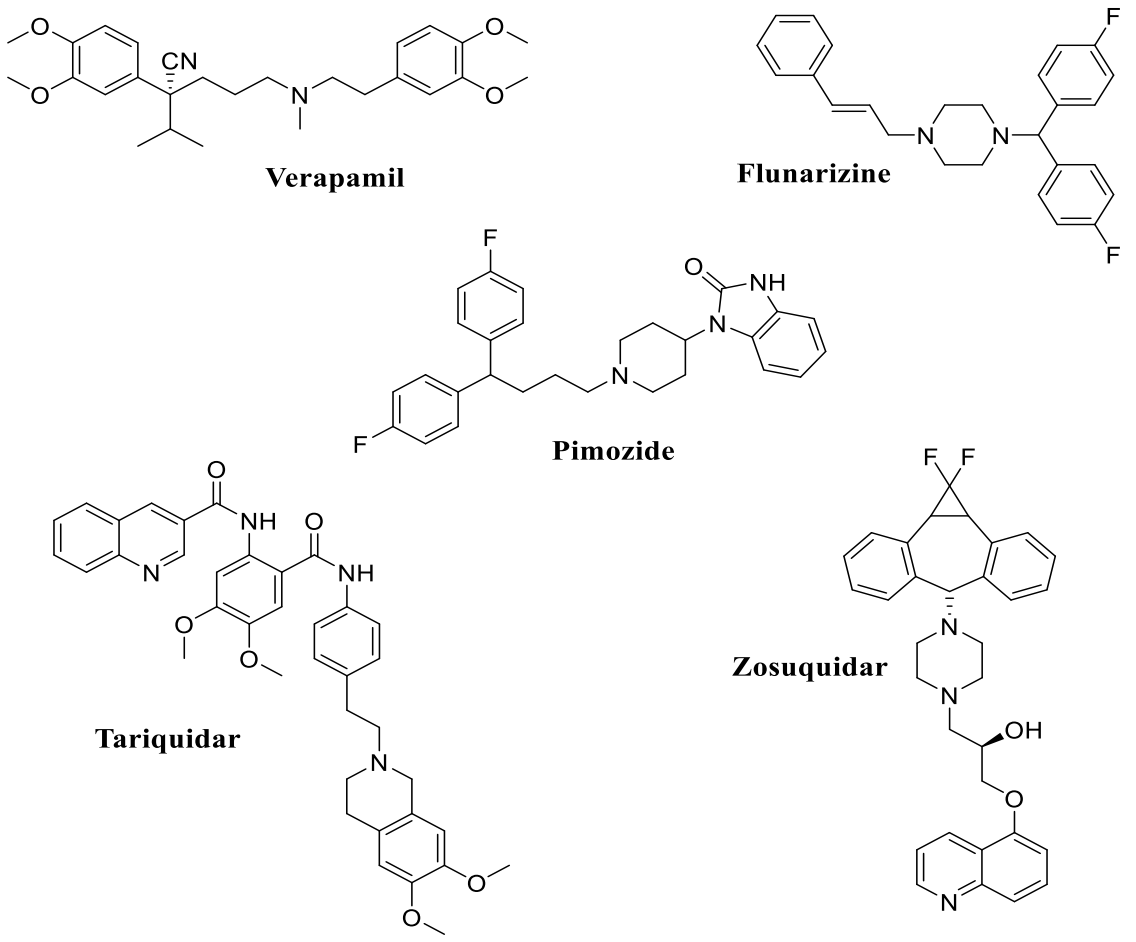

Figure 1. Representative MDR reversal agents.

However, the limited common features for the interaction of ligands with this protein have been postulated: a protonable nitrogen, aromatic rings, high lipophilicity and the ability of establishing H-bond interactions [11,16]. These data are consistent with structure-based studies performed starting from the recently published crystal structure of murine P-gp, (with 87 % sequence identity

to human P-gp) [17,18] that, despite its low resolution (3.8 Å), seem to indicate an entry pathway through the membrane bilayer. A large hydrophobic chamber of approximately 6.000 $Å^3$ was identified as a possible drug-binding pocket (DBP), near the periplasmatic lipid bilayer interface and, in the opposite side, more polar and possibly charged residues [17,19]. Therefore, besides the overall lipophilicity of the molecule, weak polar interactions, such as those produced by the overlapping of π orbitals of aromatic rings, could play an important role in stabilizing the binding of MDR reverting agents to P-gp [20].

In a previous paper [21] we described the design, synthesis and *in vitro* data for a small series of new potent inhibitors of P-gp carrying a new polycyclic scaffold, selected in view of the presence of two aromatic residues and two carbonyl groups, providing good π orbitals overlapping and having H-bond accepting properties, respectively. In particular, compound **1** (Figure 2), with a rigid but-2-ynyl side chain bearing a 3,4-dimethoxyphenetyl(methyl)amine moiety, partially related to the structure of verapamil, proved to be nearly five times more active than verapamil itself, when used at a lower dose. In a following paper [22], a series of easily affordable phenothiazine-based derivatives (Figure 2), characterized by the same but-2-ynyl spacer carrying different terminal amines, was synthesized and tested to evaluate the MDR reverting activity and antitumor profile. Some of them showed, beside an interesting reverting effect, a broad range of cellular activities, in particular the ability to induce antiproliferative effects and apoptosis on resistant cell lines, confirming the importance of the rigid but-2-ynyl amino side chain for antitumor and reverting activities. These promising results prompted us to further investigate these new classes of compounds and, in this paper, a series of new polycyclic derivatives related to **1** was designed and synthesized (**2a-e**, Figure 2 and Table 1). In particular, the polycyclic core structure was maintained and different terminal amines were inserted on the butynyl chain. Methyl- and phenylpiperazine (compounds **2d** and **2e**, respectively) were selected on the basis of the interesting results obtained with the phenothiazine series [22], and benzylpiperazine (**2c**) was chosen in order to evaluate the

role of a more flexible substituent. Moreover, considering that the lead compound **1** carried the same amine moiety found in the structure of verapamil, 1-(bis(4-fluorophenyl)methyl)piperazine (**2a**) and 1-(piperidin-4-yl)-1H-benzo[d]imidazol-2(3H)-one (**2b**) were also introduced as functional groups of flunarizine [23] and pimozide [24] (Figure 1), well known chemosensitizers. The biological profile of the new compounds, together with the lead compound **1**, was then evaluated.

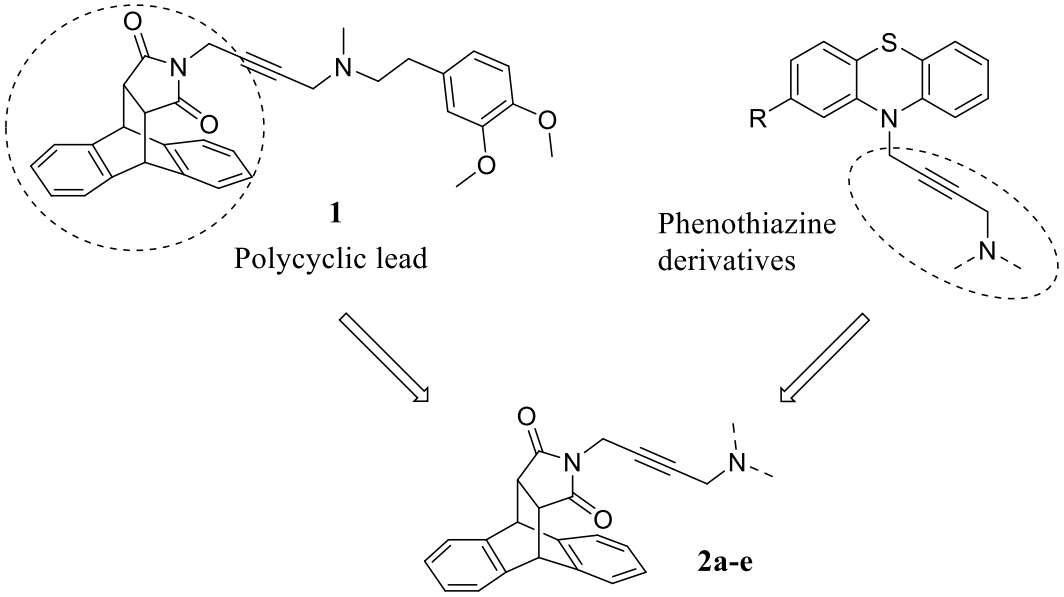

Figure 2. Design strategy for compounds **2a-e**.

2. Chemistry

All the synthesized compounds, collected in Table 1, were prepared starting from (9R,10S,11S,15R)-10,11-dihydro-9H-9,10-[3,4]epipyrroloanthracene-12,14(13H,15H)-dione, that was obtained by standard procedures [25]. According to Scheme 1, this compound was alkylated with propargyl bromide, by means of potassium *tert*-butoxide in DMSO, to give the key intermediate (9R,10S,11S,15R)-13-(prop-2-yn-1-yl)-10,11-dihydro-9H-9,10-[3,4]epipyrroloanthracene-12,14(13H,15H)-dione **3**. The final compounds **2a-e** were synthesized in

parallel by using a Carousel work-station via a readily accessible Mannich reaction, refluxing **3** with the selected amine, formaldehyde and $CuSO_4$ in ethanol/water. All the final compounds were characterized by ^{1}H- and ^{13}C-NMR, mass spectra and elemental analyses.

Scheme 1[a]

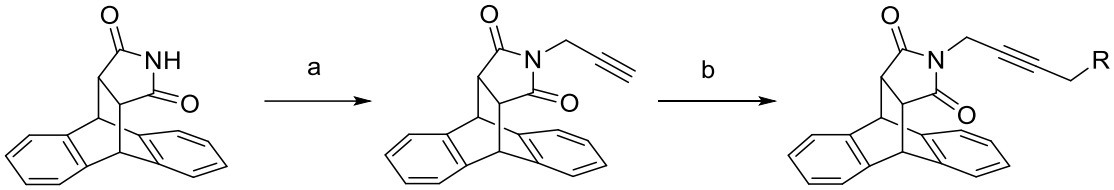

3 **2a-e**

[a]**Reagents and conditions**: a) Potassium *tert*-butoxide, propargyl bromide, DMSO, rt; (b) selected amine, formaldehyde, $CuSO_4$, $EtOH/H_2O$, reflux.

Table 1. Structures of the studied compounds.

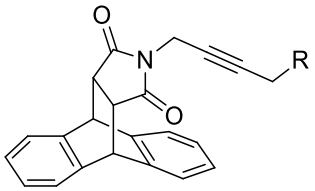

Compound	R
1[a]	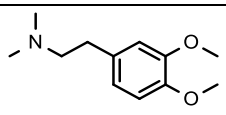

2a	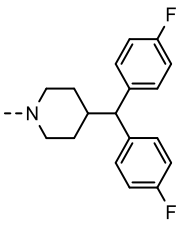
2b	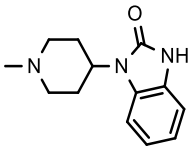
2c	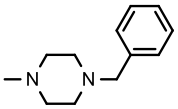
2d	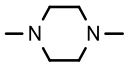
2e	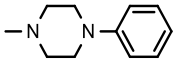

[a]See Ref. [21]

3. Biology

To evaluate the MDR reverting activity of the new compounds, a preliminary assay was performed on L5178 mouse lymphoma cells infected with pHa MDR1/A retrovirus, using rhodamine 123 as substrate and the calcium entry blocker verapamil, to which **1** is structurally related, as reference drug [26]. This model was chosen in order to have comparable results for the new derivatives, since it was previously used to assess the P-gp modulation ability of our lead compound **1** [21]. Further evaluation was then carried out by switching to a different system, i.e. the acute myeloid leukemic HL60 cells and their MDR subline (HL60R). This resistant line, obtained by continuous exposure to doxorubicin (DXR), would allow assessing the activity of the compounds in a system which most closely mimics the *in vivo* conditions of MDR phenotype. Indeed, continuous exposure to

anticancer drugs often induces the expression of different ABC efflux pumps, not only P-gp [27, 28]. Furthermore, it is well known that some of the most employed antineoplastic agents, such as doxorubicin, vinca alkaloids or metotrexate, are substrates for all these transporters [29]. We assessed the ability of the new polycyclic compounds to restore the effective intracellular concentration of DXR in the HL60R cell line; then, the mechanism of their reverting activity was investigated evaluating the ATP consumption of the cells treated with the new compounds. Indeed, substrates of ABC efflux pumps activate ATPase, whereas inhibitors are not actively transported, leaving the ATP level unchanged [30]. Moreover, the effects of the studied compounds on cell viability and cell cycle progression in the presence and in the absence of the antitumor drug were evaluated. Lead compound **1**, structurally related to the new compounds, was taken as positive control, having previously proved to be remarkably more potent than verapamil.

4. Results and discussion

As the increase in the efflux of drugs is the major feature of ABC protein mediated MDR, and considering that rhodamine efflux is more sensitive than that of anticancer drugs in P-gp models, we evaluated the efflux inhibition by the new derivatives in the transfected model with rhodamine 123 as substrate [26]. The results reported in Table 2 show that all the new compounds proved to be better MDR revertant than the reference verapamil, being the less active **2e** twice as potent as the reference and the most active **2c** 15 fold more active. For some molecules, potency was also improved with respect to compound **1**, whose previously reported MDR activity [21] proved to be nearly five times higher than verapamil, when used at a lower dose.

Table 2. Effect of compounds **2a-e** on reversal of multidrug resistance of human MDR1 gene transfected mouse lymphoma cells (rhodamine efflux test).

Compounds	Concentration (μM)	Fluorescence Activity Ratio[a]
Verapamil	4	**2.90**
	40	**5.66**
2a	0.4	**5.19**
	0.8	**8.22**
	4	**28.27**
	40	**33.38**
2b	4	**6.39**
	40	**44.6**
2c	0.4	**2.62**
	0.8	**7.76**
	4	**54.832**
	40	**85.46**
2d	4	**9.59**
	40	**64.74**
2e	4	**7.56**
	40	**11.52**

[a]Fluorescence activity ratio values were calculated by using the equation given in the experimental section.

On the basis of these preliminary data, we switched to a second model and evaluated DXR uptake on MDR leukemic cells (HL60R), obtained by continuous exposure to DXR [27], after treatment with the new derivatives. It has been reported that HL60 cells isolated for resistance to DXR mostly show an overexpression of MRP1 gene, while only a subpopulation overexpresses P-gp [28].

However, the MDR phenotype of transformed cells under selective pressure, both *in vivo* and *in vitro* systems, is due to complex biological events, leading to genetic regulation of the expression of different ABC transporters. In particular, it is hypothesized that in HL60 cells MRP1 and MDRl gene overexpression emerged in a sequential manner during selection and afterwards these two efflux pumps may be co-overexpressed [31,32]. Figure 3 shows that only compounds **2a** and **2c** were able to induce a statistically significant increase in DXR uptake in resistant cells at 10 µM, restoring intracellular levels of drug as those of the sensitive cells (HL60). Moreover, the efficacy of these new polycyclic derivatives was comparable to compound **1**. In contrast to the results seen with mouse transfected cells, these compounds did not show any appreciable activity in this model when tested at a lower dose (0.4 µM, data not shown). On the other hand, **2b**, **2d** and **2e** did not cause any increment of DXR accumulation with respect to the control (HL60R cells). Interestingly, the synthetic intermediate **3**, which was also tested to establish the role of the amine side chain, was completely devoid of activity (data not shown).

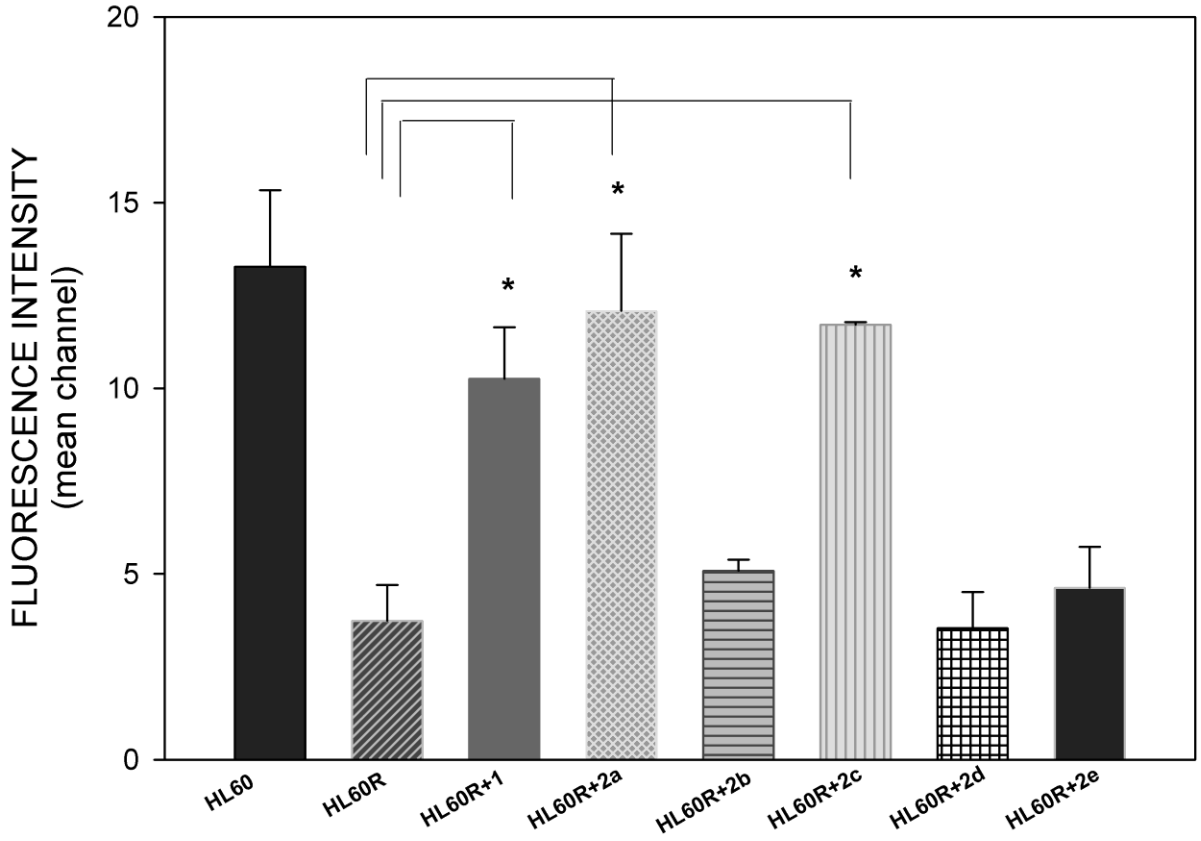

Figure 3. Influence of polycyclic compounds (10 μM) on DXR accumulation in HL60R cells. The uptake in HL60 cells is reported for comparison. Data are presented as mean ± SD determined from at least three independent experiments. Data are analysed by one-way ANOVA test *, $p<0.05$ versus HL60R.

The results obtained so far indicated that compounds **1**, **2a** and **2c** are able to inhibit drug efflux in human MDR phenotype overexpressing both MRP1 and, to a lesser extent, P-gp, as well as in the mouse transfected cells overexpressing only P-gp. Furthermore, all the compounds can be considered as substrates of ABC proteins, as their administration to HL60 R cells induced ATP consumption (see Table 2 SI).

Next, we evaluated if the new molecules could affect both HL60 and HL60R proliferation. The whole series of compounds exhibited negligible effects up to 10μM concentration on cell viability and cell cycle of both cell lines (see figures 1-4 SI). It is noteworthy that only compound **1** proved to be cytotoxic, as already observed in the previously studied L5178 cell line [21] showing higher cytotoxic activity on sensitive cells with respect to the MDR subline.

The effects due to the co-administration of polycyclic compounds plus DXR were then investigated, still keeping the concentration of 10 μM, which allowed to restore the sensitivity to DXR in the resistant subline at the same level of sensitive cells, without cytotoxicity. As expected, the increased intracellular content of DXR markedly reduced cell growth (Figure 4). In particular, **2a** and **2c**, as well as the reference compound **1**, induced cytotoxic effects, overcoming tumour drug resistance. Compounds **2d** and **2e** induced an impairment of cell growth, occurring only at 24 hours of treatment, but cell proliferation restarted in the following 24 hours, although with a lower growth rate with respect to untreated or DXR-treated cells. Surprisingly, **2b** determined a permanent arrest of cell growth**,** although it did neither induce any cytotoxic effect *per se* (as the whole series) nor increase DXR accumulation, like **2d** and **2e**.

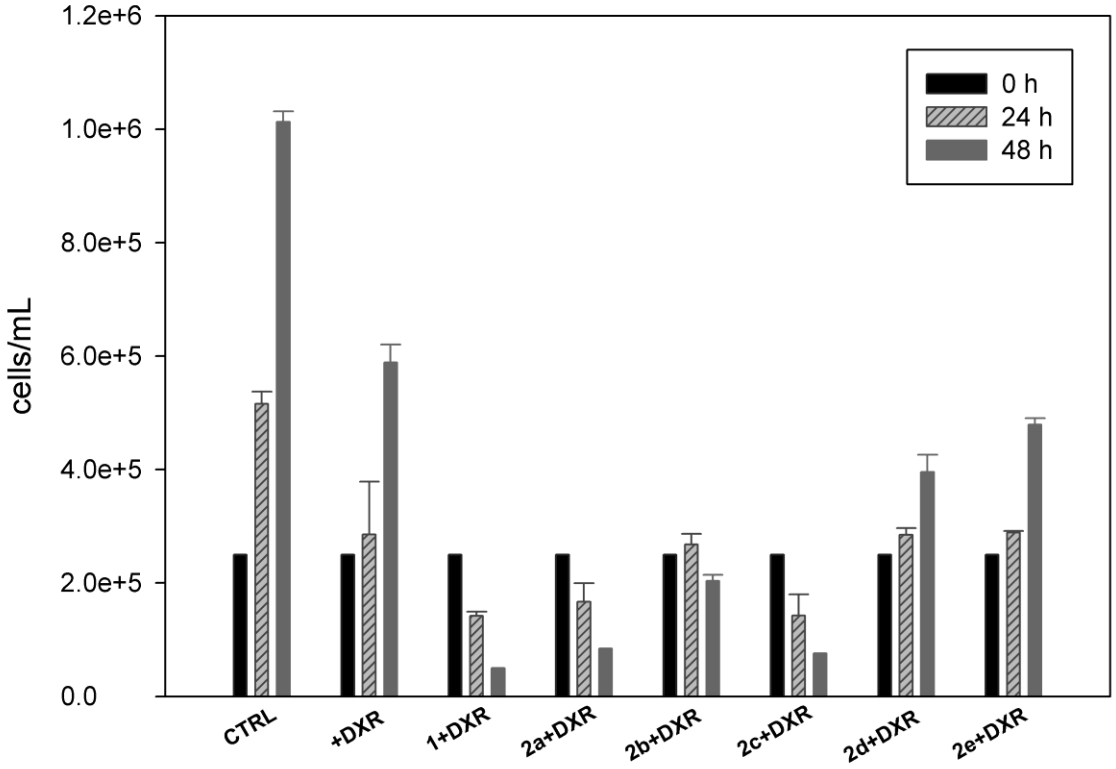

Figure 4. HL60R cell proliferation after co-administration of polycyclic derivatives (10μM) plus DXR (10 μM). The data represent mean value ± SD of at least three independent experiments.

Cell cycle analyses were also performed after the co-administration of polycyclic compounds plus DXR. As regards the revertant molecules **1**, **2a** and **2c,** an increase of recruitment in G0/G1 phase was observed after 24 hours (Figure 5), while DXR alone induced an accumulation in the G2/M phase. These results are in agreement with literature data, which showed that different intracellular DXR concentrations induce block in different cell cycle phases [33-36]. After 48 h, the massive cell death induced by DXR made the analysis of DNA profile unfeasible for the treated samples, and

morphological analysis revealed the presence of nuclear fragmentation and chromatin condensation, typical features of triggered apoptosis (Figure 5).

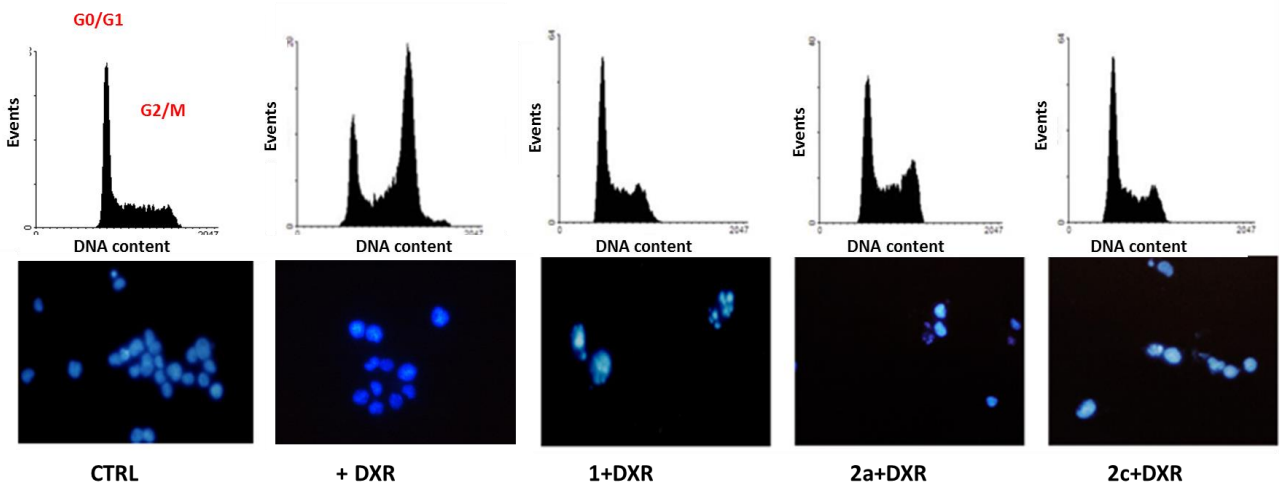

Figure 5. Cell cycle profile and morphological analysis of HL60 R co-treated with revertant compounds **1, 2a** and **2c** (10µM) plus DXR (10µM). Flow cytometric analysis of cell cycle was performed by PI staining after 24 h (upper). Morphological changes after 48 h of co-treatment with DXR were observed under fluorescence microscope by staining with HOECHST 33342 (lower). All the images have been taken at the same magnification and depict microscopic field representative of the whole cell population.

Although **2b**, **2d** and **2e** did not elicit an appreciable uptake of intracellular DXR (Figure 2), they were able to cause an accumulation in G2/M phase after 24 hours, which was more pronounced with respect to DXR alone (Figure 6). However, after 48 hours, the cells treated with **2d** and **2e** were able to exit from mitosis and proceed through the cell cycle, similarly to those treated with DXR alone. Unexpectedly, derivative **2b** caused a permanent block in G2/M phase. It is noteworthy that, among the three not revertant molecules, **2b** was the only one that affected cell proliferation in co-administration with DXR.

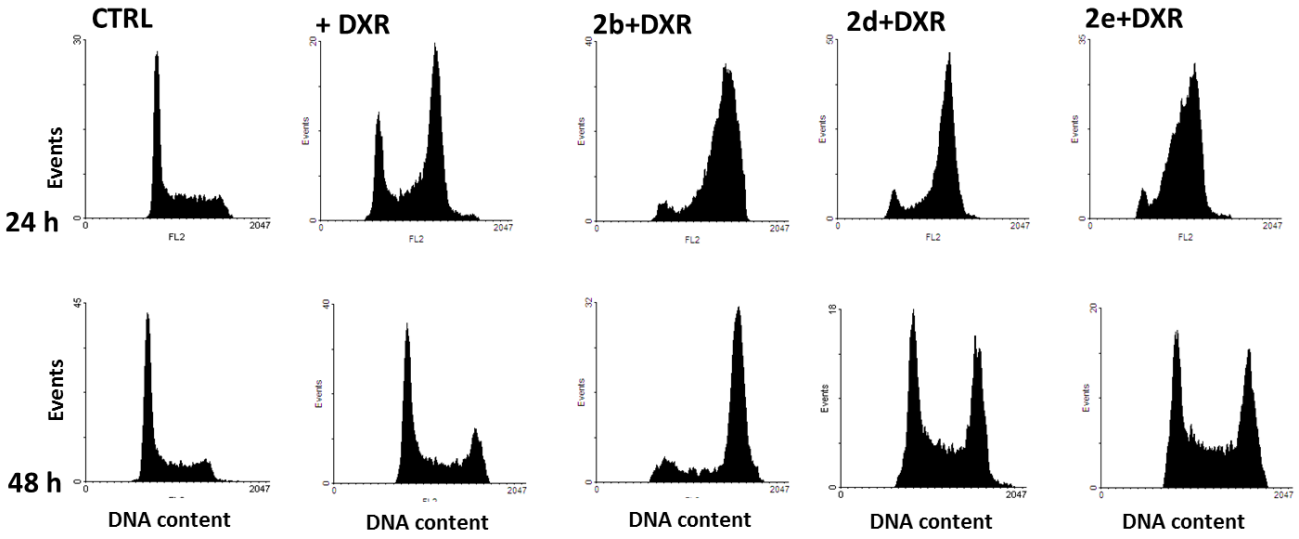

Figure 6. Cell cycle profile of HL60R cells after treatment with not revertant compounds **2b**, **2d** and **2e** (10μM) plus DXR (10 μM) for 24 and 48 hours. The figure depicts the results obtained in one experiment representative of three.

Discussing these results to obtain structure-activity relationships information, some elements could be highlighted. While both the lead compound **1** and the corresponding previously reported phenothiazines bearing verapamil side chain proved to be cytotoxic, all the new compounds showed no cytotoxicity up to 10 μM, when tested alone on HL60 cells and their MDR subline HL60R.

Thus, the presence of verapamil amino side chain conferred a marked cytotoxic effect when appended to both the phenothiazine and the polycyclic core structures, while no appreciable toxicity was seen with the newly introduced amino side chains. Nevertheless, the cytotoxic effect of compound **1** was significantly lower on HL60R with respect to sensitive cells and did not hamper its evaluation as chemosensitizer, in view of its potent MDR reverting activity. Furthermore, in the previously studied phenothiazine series, different levels of cytotoxicity had been found with most of the derivatives, including those carrying the side chains introduced in these new polycyclic compounds, so that reverting activity could not be evaluated for some of them. The results here reported suggest that the toxicity could thus be related to the phenothiazine core, rather than the side chains.

As far as MDR reverting activity is concerned, while all the new compounds proved to be potent P-gp modulators, the introduction of methyl- and phenylpiperazine on the polycyclic scaffold did not lead to the same interesting results obtained with the corresponding phenothiazines, being **2d** and **2e** unable to restore cell sensitivity to DXR in the MDR phenotype HL60R. Remarkably, the substitution of phenylpiperazine with benzylpiperazine (**2c**) led to a potent reverting agent, both in the rhodamine efflux test and in the DXR uptake assay, showing this compound to interact with both P-gp and MRP1 efflux pumps. This marked difference in activity, obtained with a small modification of the side chain, could be due to an increase in flexibility leading to a better fit in the binding pocket of these proteins. The introduction of another phenyl ring on the side chain led to compound **2a**, carrying the bulky functional fluorinated substituent of flunarizine, which also proved to possess high reverting activity, suggesting that this amino function could provide additional interactions with the target. It is noteworthy that the logP of this compound (6.30) is quite higher than the rest of the series, whose values ranged from 2.54 to 4.61. In this context, it could be noted that, as expected, compounds **2b** and **2d**, having the lower logP values are also the least active. Moreover, the role of the amine side chain is indeed crucial, as confirmed by the absence of activity of the synthetic intermediate **3**. These observations are in agreement with the

features required for interaction of ligands with ABC proteins, as well as the recently reported crystallographic requirements for P-gp [17].

5. Conclusions

Starting from the potent P-gp modulator **1**, bearing a novel polycyclic scaffold, and taking into account the biological activities of a following series of phenothiazine derivatives, new polycyclic molecules were designed and synthesized, and the MDR reverting profile was evaluated on two different experimental models, the mouse lymphoma cells transfected with the MDR1 gene, and the MDR phenotype HL60R. Derivatives **2a** and **2c** and the lead compound **1** proved to be the most interesting molecules, being able to interfere with different ABC proteins involved in chemotherapy resistance. The new derivatives **2a** and **2c** did not show any cytotoxicity when tested alone on both HL60 and HL60R cell lines, while an arrest in G0/G1 phase and a massive apoptotic effect was observed when co-administrated with DXR. Based on these results, **2a** and **2c** could be regarded as non-toxic new potential chemosensitizers. An intriguing pattern of antiproliferative activities arised with the co-administration of DXR and compounds **2b**, **2d** and **2e**. These weak revertant molecules were able to induce a block in G2/M, potentiating DXR effect, after 24 h of treatment and, while this effect proved to be reversible for DXR, **2d** and **2e**, the co-administration of DXR with the not-cytotoxic compound **2b** led to a permanent arrest in G2/M. This unexpected finding will be the subject of further investigations aimed at the elucidation of this peculiar behaviour.

Finally, the confirmed intrinsic cytotoxic activity of compound **1** together with the revertant activity observed in this study could broaden its antitumor applications. Taken together, these results seem to indicate in the polycyclic core of this class of compounds a potential new privileged structure in medicinal chemistry.

6. EXPERIMENTAL SECTION

6.1. Chemistry. General Methods. Starting materials, unless otherwise specified, were used as high grade commercial products. Solvents were of analytical grade. Reaction progress was followed by thin layer chromatography (TLC) on precoated silica gel plates (Merck Silica Gel 60 F254) and then visualized with a UV254 lamplight. Chromatographic separations were performed on silica gel columns by flash method (Kieselgel 40, 0.040-0.063 mm, Merck). Melting points were determined in open glass capillaries, using a Büchi apparatus and are uncorrected. ^{1}H NMR and ^{13}C NMR spectra were recorded on a Varian Gemini spectrometer 400MHz, and chemical shifts (δ) were reported as parts per million (ppm) values relative to tetramethylsilane (TMS) as internal standard; coupling constants (*J*) are reported in Hertz (Hz). Standard abbreviations indicating spin multiplicities are given as follow: s (singlet), d (doublet), t (triplet), br (broad), q (quartet) or m (multiplet). Mass spectra were recorded on Waters ZQ 4000 apparatus operating in electrospray mode (ES). Chemical purities of tested compounds were determined by elemental analysis (C, H, N) and were within ± 0.4 % of the theoretical values.
Compounds were named relying on the naming algorithm developed by CambridgeSoft Corporation and used in Chem-BioDraw Ultra 12.0.

6.2. General parallel procedure for the synthesis of the Mannich bases (2a-e)

A suspension of formaldehyde (0.21 mL, 2 mmol), the selected amine (2 mmol), and $CuSO_4$ (0.05 g) was added to distinct reactors containing a water/ethanol 1:1 solution (10 mL) of the previously described (9R,10S,11S,15R)-13-(prop-2-yn-1-yl)-10,11-dihydro-9H-9,10-[3,4]epipyrroloanthracene-12,14(13H,15H)-dione **3** [25] (0.63 g, 2 mmol) and the mixture was heated to reflux for 24 h. After cooling, ammonium hydroxide solution (15 mL) was added and the mixture was extracted with diethylether (3 x 20 mL), the organic layers were dried over anhydrous

Na_2SO_4 and evaporated to give an oily crude which was purified by flash column chromatography on silica gel using a suitable eluent and/or by crystallization. The compounds were obtained with yields ranging from 30 to 65 %. Where indicated, the oxalate salt was prepared dissolving the compound in ethanol and adding an equimolar amount of oxalic acid. After stirring for 30 min at rt, the mixture was filtered and diethyl ether was slowly added to the solution until crystallization occurred.

6.2.1. (9R,10S,11S,15R)-13-(4-(4-(bis(4-fluorophenyl)methyl)piperazin-1-yl)but-2-yn-1-yl)-10,11-dihydro-9H-9,10-[3,4]epipyrroloanthracene-12,14(13H,15H)-dione (2a). Eluent: toluene/acetone 4:1. Yield 40 %. M.p. 187-189 °C (ethanol). ^{1}H NMR: δ 2.25-2.40 (m, 4H), 2.45-2.55 (m, 4H), 3.10 (s, 2H), 3.21 (s, 2H), 3.80 (s, 2H), 4.18 (s, 1H), 4.78 (s, 2H), 6.93-7.07 (m, 4H, arom), 7.08-7.15 (m, 2H, arom), 7.17-7.20 (m, 2H, arom), 7.21-7.24 (m, 2H, arom), 7.31-7.36 (m, 6H, arom). ^{13}C NMR: δ 27.6, 45.3, 46.8, 46.8, 74.4, 77.5, 115.2, 115.5, 124.2, 124.9, 126.7, 126.9, 129.2, 129.2, 138.1, 138.2, 138.4, 141.3, 160.5, 162.9, 175.5. ES-MS (*m/z*): 636 ($M+Na^+$). Anal. $C_{39}H_{33}F_2N_3O_2$ (C, H, N).

6.2.2. (9R,10S,11S,15R)-13-(4-(4-(2-oxo-2,3-dihydro-1H-benzo[d]imidazol-1-yl)piperidin-1-yl)but-2-yn-1-yl)-10,11-dihydro-9H-9,10-[3,4]epipyrroloanthracene-12,14(13H,15H)-dione (2b). Eluent: toluene/acetone 4:1. Yield 30 %. M.p. 203 °C dec. (ethanol). ^{1}H NMR: δ 1.80-1.87 (m, 6H), 2.43-2.48 (m, 4H), 3.23 (s, 4H), 3.78 (s, 2H), 4.78 (s, 2H), 7.05-7.17 (m, 6H, arom), 7.24-7.26 (m, 4H, arom), 7.35-7.37 (m, 2H, arom). ^{13}C NMR: δ 27.2, 45.4, 47.0, 57.9, 70.7, 76.7, 108.0, 124.25, 124.9, 126.8, 126.9, 127.1, 138.3, 141.3, 175.5, 221.5. ES-MS (*m/z*): 565 ($M+Na^+$). Anal. $C_{34}H_{30}N_4O_3$ (C, H, N).

6.2.3. (9R,10S,11S,15R)-13-(4-(4-benzylpiperazin-1-yl)but-2-yn-1-yl)-10,11-dihydro-9H-9,10-[3,4]epipyrroloanthracene-12,14(13H,15H)-dione (2c). Eluent: dichloromethane/ethyl acetate

7:3. Yield 35 %. M.p. (oxalate) 209-211 °C. ^{1}H NMR: δ 2.39-2.46 (m, 8H), 3.09 (s, 2H), 3.21 (s, 2H), 3.48 (s, 2H), 3.78 (s, 2H), 4.77 (s, 2H), 7.06-7.08 (m, 2H, arom), 7.14-7.16 (m, 2H, arom), 7.22-7.29 (m, 7H, arom), 7.34-7.36 (m, 2H, arom). ^{13}C NMR: δ 27.6, 45.4, 46.9, 46.9, 52.0, 52.9, 63.0, 76.7, 77.73, 124.23, 124.93, 126.7, 126.9, 127.0, 128.2, 129.3, 137.9, 138.4, 141.4, 175.5. ES-MS (*m/z*): 524 ($M+Na^+$). Anal. $C_{33}H_{31}N_3O_2$ (C, H, N).

6.2.4. (9R,10S,11S,15R)-13-(4-(4-methylpiperazin-1-yl)but-2-yn-1-yl)-10,11-dihydro-9H-9,10-[3,4]epipyrroloanthracene-12,14(13H,15H)-dione (2d). Eluent: dichloromethane/ethyl acetate 7:3. Yield: 45 %. M.p. (oxalate) 202-205 °C. ^{1}H NMR: δ 2.20-2.24 (m, 4H) 2.25 (s, 3H), 2.40-2.65 (m, 4H), 3.15 (s, 2H), 3.24 (s, 2H), 3.80 (s, 2H), 4.75 (s, 2H), 7.10-7.18 (m, 4H, arom), 7.22-7.39 (m, 4H, arom). ^{13}C NMR: δ 28.0, 45.8, 45.9, 46.2, 47.2, 47.4, 47.5, 52.2, 55.3, 77.9, 124.7, 125.3, 125.4, 127.2, 127.2, 127.3, 127.5, 138.9, 141.8, 176.0. ES-MS (*m/z*): 448 ($M+Na^+$). Anal. $C_{27}H_{27}N_3O_2$ (C, H, N).

6.2.5. (9R,10S,11S,15R)-13-(4-(4-phenylpiperazin-1-yl)but-2-yn-1-yl)-10,11-dihydro-9H-9,10-[3,4]epipyrroloanthracene-12,14(13H,15H)-dione (2e). Crystallized from toluene. Yield: 45 %. M.p. 241 °C dec. (ethanol). ^{1}H NMR δ 2.52-2.65 (m, 4H), 3.19-3.22 (m, 6H), 3.24 (s, 2H), 3.83 (s, 2H), 4.80 (s, 2H), 6.85-6.95 (m, 3H, arom), 7.10-7.20 (m, 4H, arom), 7.25-7.40 (m, 6H, arom). ^{13}C NMR: δ 28.2, 46.0, 47.5, 47.7, 49.6, 52.6, 78.0, 116.7, 120.4, 124.8, 125.6, 127.4, 127.5, 129.7, 139.1, 142.0, 151.8, 176.1. ES-MS (*m/z*): 510 ($M+Na^+$). Anal. $C_{32}H_{29}N_3O_2$ (C, H, N).

6.3. Biological methods.

6.3.1. Reagents. All reagents were from Sigma Aldrich (St. Louis, Mo, USA) if not specifically stated, and were Ultrapure grade.

6.3.2. Cell culture and treatment. The L5178 mouse T-cell lymphoma cells were transfected with pHa MDR1/A retrovirus. MDR1-expressing cell lines were selected by culturing the infected cells with 60 ng/mL colchicine to maintain the expression of the MDR phenotype.

L5178 (parent) mouse T-cell lymphoma cells and the human MDR1-transfected subline were cultured in McCoy's 5A medium supplemented with 10% heat-inactivated horse serum, L-glutamine and antibiotics.

Human promyelocytic leukemic cell line HL60 was purchased from American Type Culture Collection (ATCC,Manassas, VA) and its MDR subline resistant to doxorubicin (HL60/DXR) was kindly provided by ML. Dupuis (Istituto Superiore di Sanità, Roma,Italy). Cells were cultured in RPMI 1640 medium supplemented with 2mM L-glutamine, 10 % heat-inactivated foetal bovine serum, L-glutamine and antibiotics. Every ten passages HL60R were treated with doxorubicin (DXR) 1μg/mL to maintain drug resistance. All the polycyclic derivatives were dissolved in DMSO and used at the final concentration of 10μM.

6.3.3. Rhodamine -123 efflux assay. *Assay for reversal of MDR1 in mouse lymphoma cells.* The L5178 MDR and L5178Y parent cells, grown in complete McCoy's 5A, were resuspended in serum-free McCoy's 5A medium to a density of 2×10^6/mL and distributed in 0.5-mL aliquots into Eppendorf centrifuge tubes. The tested compounds were added at various concentrations (0.4 - 40 μM) of the 1.0-10.0 mg/mL stock solutions and the samples were incubated for 10 min. at room temperature. Next, 10 μL (5.2 μM final concentration) of the indicator rhodamine-123 (Sigma, St Louis, MO, USA) was added to the samples and the cells were incubated for a further 20 min at 37 °C, washed twice and resuspended in 0.5 mL PBS for analysis. The fluorescence of the cell population was measured with a Beckton Dickinson FACScan flow cytometer. Verapamil (EGIS, Hungarian Pharmaceutical Company, Budapest, Hungary) was used as a positive control in the rhodamine-123 exclusion experiments. The percentage mean fluorescence intensity was calculated

for the treated MDR and parental cell lines as compared with the untreated cells. An activity ratio R was calculated via the following equation on the basis of the measured fluorescence values:

$$R = \frac{MDR\,treated / MDR\,control}{parental treated / parental control}$$

6.3.4. Determination of DXR accumulation. HL60 and HL60R cells, adjusted at 2.5×10^5 cells/mL, were exposed to 10 µM of the polycyclic compounds for 2 hours and then to DXR (10 µM) for 2 hours. Cells were then washed twice in cold PBS, resupended in fresh medium at the concentration of $1x10^6$ cells/mL. The anthracycline fluorescence was immediately examined by using a Brite HS (BioRad, UK) cytometer, equipped with Hg lamp and a filter set with an excitation band centered at 488 nm and the emission band centered at 600 nm, and the emitted fluorescence intensity was acquired on a logarithmic scale.

6.3.5. ATP consumption assay. Bioluminescence ATP measurement was performed according to the manufacturers protocol of the Ultrasnap ATP test. The assay is based on the production of light caused by the reaction of ATP with added luciferase and d-luciferin (substrate solution), and the amount of light emitted is proportional to the ATP concentration. HL60R cells, adjusted at 2.5×10^5 cells/mL, were exposed to 10 µM of the polycyclic compounds for 2 hours in a humidified atmosphere containing 5% CO_2 at 37 °C. Samples were then washed twice in cold PBS and finally resuspended at the concentration of $1x10^6$ cells/mL. To allow cell lysis 1 x 10^5 cells were put into Ultrasnap swab and agitated for 20 s. The luminescence was measured by System Sure II luminometer (Hygiena).

6.3.6. Cell proliferation assay. HL60R cells were seeded at the density of $1.5x10^5$ cells/mL. After 24 hours, they were exposed to the polycyclic compounds (10µM) for 2 hours and then to 10 µM DXR. The viable cells were counted by using a Bürker haemocytometer in the presence of Trypan Blue after 24 and 48 hours.

6.3.7. Cell cycle analysis. To perform the cell cycle analysis HL60R cells were treated with polycyclic compounds plus 10 μM DXR for 24 and 48 hours. After the incubation, cells were fixed by 70 % ice-cold ethanol and left at -20 °C overnight. After centrifugation pellets were resuspended in an appropriate volume (0.5 - 2 mL) of staining solution (PBS, 5μg/mL Propidium Iodide and 10μg/mL DNAse free RNase A). Samples were incubated in the dark for 30 min at 37 °C and analyzed by flow cytometry, acquiring the red fluorescence of PI on a linear scale at 600 nm.

6.3.8. Fluorescence Microscopy. The cells were centrifuged onto slides by a cytospin (150 g, 5 min), then were washed twice with PBS, fixed with 4 % paraformaldehyde in PBS and permeabilized with 0.5 % Triton X-100 in PBS for 5 min at 4 °C. After 2 washes in PBS, sample were incubated in presence of Hoechst 33432 0,1 mg/mL, washed and analyzed by fluorescence microscopy.

6.3.9. Statistical analysis. The experiments were repeated at least three times, and the values were reported as mean ± standard deviation. To determine the significant revertant activity of polycyclic compounds a one-way ANOVA analysis was performed. Values of $p < 0.05$ were taken to be statistically significant.

Supplementary data

Effects of the studied compounds on HL60 and HL60R proliferation and cell cycle; statistical analysis of DXR accumulation assay, evaluation of ATP consumption, representative NMR spectra.

Acknowledgments

This work was financially supported by a PRIN2009 Project Grant from MIUR, Italy.

Abbreviations used

ABC, ATP-binding cassette; ATP, adenosine-5′-triphosphate; Bcl-2, B-cell lymphoma-2; CDKs, cycline-dependent kinases; DBP, drug-binding pocket; DXR, doxorubicin; IAPs, inhibitors of apoptotic proteins; MDR, multidrug resistance; MRP1, multidrug resistance protein-1; NBD, nucleotide-binding domain; P-gp, P-glycoprotein; GS-X pump, glutathione S-conjugate export pump; TMD, transmembrane domains.

References

[1] M. De Falco, A. De Luca, Cell Cycle as a Target of Antineoplastic Drugs, Curr. Pharm. Des. 16 (2010) 1417-1426.

[2] S. Diaz-Moralli, M. Tarrado-Castellarnau, A. Miranda, M. Cascante, Targeting cell cycle regulation in cancer therapy, Pharm. Ther. 138 (2013) 255–271.

[3] M. Tomeka, T. Akiyama, C.R. Dass, Role of Bcl-2 in tumour cell survival and implications for pharmacotherapy, J. Pharm. Pharmacol. 64 (2012) 1695–1702.

[4] M. Saleem, M.I. Qadir, N. Perveen, B. Ahmad, U. Saleem, T. Irshad, B. Ahmad, Inhibitors of apoptotic proteins: new targets for anticancer therapy, Chem. Biol. Drug Des. 82 (2013) 243–251.

[5] S. Nobili, I. Landini, T. Mazzei, E. Mini, Overcoming tumor multidrug resistance using drugs able to evade P-Glycoprotein or to exploit its expression, Med. Res. Rev. 32 (2012) 1220-1262.

[6] K.M. Giacomini, S.M. Huang, D.J. Tweeie, L.Z. Benet, K.L. Brouwer, X. Chu, A. Dahlin, R. Evers, V. Fischer, K.M. Hillgren, K.A. Hoffmaster, T. Ishikawa, D. Keppler, R.B. Kim, C.A. Lee, M. Niemi, J.W. Polli, Y. Sugiyama, P.W. Swaan, J.A. Ware, S.H. Wright, S.W.

Yee, M.J. Zamek-Gliszczynski, L. Zhang, Membrane transporters in drug development, Nat. Rev. Drug Discov. 9 (2010) 215-236.

[7] W.D. Stein, Kinetics of the multidrug transporter (P-glycoprotein) and its reversal, Physiol. Rev. 77 (1997) 545-590.

[8] A.C. Rabello de Moraes, C.K. Maranho, G.S. Rauber, M.C. Santos-Silva, Importance of detecting multidrug resistance proteins in acute leukemia prognosis and therapy, J. Clin. Lab. Anal. 27 (2013) 62-71.

[9] R.H. Ho, R.B. Kim, Transporters and drug therapy: Implications for drug disposition and disease, Clin. Pharm. Ther. 78 (2005) 260–277.

[10] N.A. Colabufo, F. Berardi, M. Contino, M. Niso, R. Perrone, ABC pumps and their role in active drug transport, Curr. Top. Med. Chem. 9 (2009) 119−129.

[11] I.K. Pajeva, C. Globisch, M. Wiese, Combined pharmacophore modeling, docking, and 3D QSAR studies of ABCB1 and ABCC1 transporter inhibitors, Chem. Med. Chem. 4 (2009) 1883–1896.

[12] M. Saraswathy, S. Gong, Different strategies to overcome multidrug resistance in cancer, Biotechnol. Adv. 31 (2013) 1397-1407.

[13] N. A. Colabufo, F. Berardi, M. Cantore, M. Contino, C. Inglese, M. Niso, R. Perrone, Perspective of P-glycoprotein modulating agents in oncology and neurodegenerative diseases: pharmaceutical, biological, and diagnostic potentials, J. Med. Chem. 53 (2010) 1883-1897.

[14] P. Mistry, A.J. Stewart, W. Dangerfield, S. Okiji, C. Liddle, D. Bootle, J.A. Plumb, D. Templeton, P. Charlton, In vitro and in vivo reversal of P-glycoprotein-mediated multidrug resistance by a novel potent modulator, XR9576, Cancer Res. 61 (2001) 749-758.

[15] A.H. Dantzig, R.L. Shepard, J. Cao, K.L. Law, W.J. Ehlhardt, T.M. Baughman, T.F. Bumol, J.J. Starling, Reversal of P-glycoprotein-mediated multidrug resistance by a potent cyclopropyldibenzosuberane modulator, LY335979, Cancer Res. 56 (1996) 4171-4179.

[16] V. Poongavanam, N. Haider, G.F. Ecker, Fingerprint-based in silico models for the prediction of P-glycoprotein substrates and inhibitors, Bioorg. Med. Chem. 20 (2012) 5388–5395.

[17] S.G. Aller, J. Yu, A. Ward, Y. Weng, S. Chittaboina, R. Zhuo, P.M. Harrell, Y.T. Trinh, Q. Zhang, I.L. Urbatsch, G. Chang, Structure of P-Glycoprotein reveals a molecular basis for poly-specific drug binding, Science 323 (2009) 1718-1722.

[18] M.S. Jin, M.L. Oldham, Q. Zhang, J. Chen, Crystal structure of the multidrug transporter P-glycoprotein from Caenorhabditis elegans, Nature 490 (2012) 566-570.

[19] F.J. Sharom, The P-glycoprotein multidrug transporter, Essays Biochem. 50 (2011) 161−178.

[20] G. Klopman, L.M. Shi, A. Ramu, Quantitative structure-activity relationships of multidrug reversal agents, Mol. Pharm. 52 (1997) 323–334.

[21] A. Bisi, S. Gobbi, A. Rampa, F. Belluti, L. Piazzi, P. Valenti, N. Gyemant, J. Molnár, New potent P-glycoprotein inhibitors carrying a polycyclic scaffold, J. Med. Chem. 49 (2006) 3049–3051.

[22] A. Bisi, M. Meli, S. Gobbi, A. Rampa, M. Tolomeo, L. Dusonchet, Multidrug resistance reverting activity and antitumor profile of new phenothiazine derivatives, Bioorg. Med. Chem. 16 (2008) 6474–6482.

[23] B.T. Hill, L.K. Hosking, Differential effectiveness of a range of novel drug-resistance modulators, relative to verapamil, in influencing vinblastine or teniposide cytotoxicity in human lymphoblastoid CCRF-CEM sublines expressing classic or atypical multidrug resistance, Cancer Chemother. Pharmacol. 33 (1994) 317–324.

[24] T. Litman, T. Zeuthen, T. Skovsgaard, W.D. Stein, Structure-activity relationships of P-glycoprotein interacting drugs: kinetic characterization of their effects on ATPase activity, Biochim. Biophys. Acta 1361 (1997) 159–168.

[25] S. Bova, S. Saponara, A. Rampa, S. Gobbi, L. Cima, F. Fusi, G. Sgaragli, M. Cavalli, C. de los Rios, J. Striessnig, A. Bisi, Anthracene based compounds as new L-type Ca^{2+} channel blockers: design, synthesis, and full biological profile, J. Med. Chem. 52 (2009) 1259-1262.

[26] J.S. Lee, K. Paull, M. Alvarez, C. Hose, A. Monks, M. Grever, A.T. Fojo, S.E.Bates, Rhodamine efflux patterns predict P-glycoprotein substrates in the National Cancer Institute drug screen, Mol. Pharmacol. 46 (1994) 627-638.

[27] A. Ascione, M. Cianfriglia, M.L. Dupuis, A. Mallano, A. Sau, F. Pellizzari Tregno, S. Pezzola, A.M. Caccuri, The glutathione S-transferase inhibitor 6-(7-nitro-2,1,3-benzoxadiazol-4-ylthio) hexanol overcomes the MDR1-P-glycoprotein and MRP1-mediated multidrug resistance in acute myeloid leukemia cells, Cancer Chemother. Pharmacol. 64 (2009) 419-424.

[28] M. Cianfriglia, A. Mallano, A. Ascione, M.L. Dupuis, Multidrug transporter proteins and cellular factors involved in free and mAb linked calicheamicin-gamma1 (gentuzumab ozogamicin, GO) resistance and in the selection of GO resistant variants of the HL60 AML cell line, Int. J. Oncol. 36 (2010) 1513-1520.

[29] D. Kostrzewa-Nowak, B. Bieg, M.J. Paine, C.R. Wolf, J. Tarasiuk, The role of bioreductive activation of antitumour anthracycline drugs in cytotoxic activity against sensitive and multidrug resistant leukaemia HL60 cells, Eur. J. Pharmacol. 674 (2012) 112-125.

[30] L. Zinzi, E. Capparelli, M. Cantore, M. Contino, M. Leopoldo, N. A. Colabufo, Small and innovative molecules as new strategy to revert MDR, Front. Oncol. 4 (2014) 1-12

[31] I. Brock, D.R. Hipfner, B.S. Nielsen, P.B. Jensen, R.G. Deeley, S.P.C. Cole, M. Shested, Sequential coexpression of the multidrug resistance gene MRP and mdr1 and their

products in VP-16 (etoposide)-selected H69 small cell lung cancer cells, Cancer Res. 55 (1995) 459-462.

[32] D.C. Zhou, S. Ramond, F. Viguie, A.M. Faussat, R. Zittoun, J.P. Marie, Progressive resistance to homoharringtonine in human myeloleukemia K562 cells: relationship to sequential emergence of MRP and MDR1 gene overexpression and MDR1gene translation, Int. J. Cancer 65 (1996) 365-371.

[33] R. Nowak, J. Tarasiuk, Anthraquinone antitumour agents, doxorubicin, pirarubicin and benzoperimidine BP1, trigger caspase-3/caspase-8-dependent apoptosis of leukaemia sensitive HL60 and resistant HL60/VINC and HL60/DOX cells, J. Anticancer Drugs 23 (2012) 380-392.

[34] R. Nowak, J. Tarasiuk, Retaining cytotoxic activity of anthrapyridone CO1 against multidrug resistant cells is related to the ability to induce concomitantly apoptosis and lysosomal death of leukaemia HL60/VINC and HL60/DOX cells, J. Pharm. Pharmacol. 65 (2013) 855-867.

[35] D.A. Gewirtz, A critical evaluation of the mechanisms of action proposed for the antitumor effects of the anthracycline antibiotics adriamycin and daunorubicin, Biochem. Pharmacol. 57 (1999) 727-741.

[36] R. Lupertz, W. Wätjen, R. Kahl, Y. Chovolou, Dose- and time-dependent effects of doxorubicin on cytotoxicity, cell cycle and apoptotic cell death in human colon cancer cells, Toxicology 271 (2010*)* 115-121.